www.project-foci.eu

Co-funded by
the European Union

UK Research
and Innovation

Horizon Europe

(HORIZON-CL5-2021-D1-01)

Non-CO2 Forcers and their Climate, Weather, Air Quality and Health Impacts

FOCI

Deliverable 3.1

Model improvements for physico-chemical processes of non-CO2 radiative forcers

Grant agreement No 101056783

Grant Agreement No.	101056783	
Project acronym	FOCI	
Project full title	Non-CO2 Forcers and their Climate, Weather, Air Quality and Health Impacts	
Call	HORIZON-CL5-2021-D1-01	
Deliverable name	D3.1 Model improvements for physico-chemical processes of non-CO2 radiative forcers	
WP contributing to the deliverable	WP3 Improvements in Earth System Modelling for climate applications	
Task producing the deliverable	Task 3.1 Physico-chemical processes of non-CO2 radiative forcers	
Type	X	Report
		Prototype
		Demonstrator
		Other: Data
Dissemination level	X	Public
		Sensitive
		UE/EU-Restricted
Due date of deliverable	Month 30	
Actual submission date	Month 30	
Lead beneficiary	KNMI	
Author(s)	Twan van Noije (KNMI), Lianghai Wu (KNMI), Philippe Le Sager (KNMI), Vincent Huijnen (KNMI), Tommi Bergman (FMI), Harri Kokkola (FMI), Anton Laakso (FMI), Oriol Jorba (BSC), María Gonçalves-Ageitos (BSC), Marios Chatziparaschos (BSC), Montserrat Costa Surós (BSC), Sergey Gromov (MPI-C), Andrea Pozzer (MPI-C)	
Other Contributor(s)	Ranjeet Sokhi (UH)	
Reviewer(s)	Sandro Finardi (ARIANET)	
Keywords	FOCI, deliverables, model improvements	

ACKNOWLEDGEMENTS

This project has been co-funded by the European Union with funding from the European Union's Horizon Europe research and innovation programme under grant agreement No. 101056783 and from UKRI under the UK Government's Horizon Europe Guarantee (UKRI Reference Numbers: 10040465, 10053814 and 10050799).

Version	Date	Modified by	Comments
0.0	20 Jan 2025	Twan van Noije	First draft shared with co-authors
1.0	5 Feb 2025	Twan van Noije and co-authors	Complete version with input from co-authors shared with reviewer
2.0	21 Feb 2025	Twan van Noije and Sergey Gromov	Revisions made to incorporate reviewer's comments
3.0	27 Feb 2025	Twan van Noije	Final version

	Name	Date
Verification Final Draft by WP leaders	Oriol Jorba (BSC), Twan van Noije (KNMI)	27 Feb 2025
Check before upload by project Coordinator	Tomas Halenka (CU)	3 March 2025

TABLE OF CONTENTS

EXECUTIVE SUMMARY

This document is the deliverable “D3.1: Model improvements for physico-chemical processes of non-CO2 radiative forcers” for the European Union project “FOCI: Non-CO2 Forcers and their Climate, Weather, Air Quality and Health Impacts” (hereinafter also referred to as FOCI, project reference: 101056783).

The report describes the development and integration of a new aerosol scheme in EC-Earth4 and the implementation of improvements for physico-chemical processes of non-CO2 radiative forcers in EC-Earth4 and EMAC. In addition to the upgrade from IFS 36r4 to OpenIFS 48r1 bringing a major improvement in terms of the representation of the general circulation, the development activities introduced in this Deliverable have improved the treatment of multiple physico-chemical processes compared to how these were described in previous EC-Earth3. The most noteworthy improvements are an updated description of aerosol wet scavenging, both in and below clouds, a more direct computation of longwave radiative properties of tropospheric aerosols; the introduction of an improved activation scheme; an updated tropospheric chemical mechanism, and the addition of a comprehensive stratospheric chemistry scheme. Concerning the EMAC, this Deliverable describes the developments accomplished within the project aimed at the improved EMAC representation of tropospheric sulphate formation. These include implementation of comprehensive kinetic chemistry of sulfuric acid formation from natural precursors and relevant intermediates, and of the new particle formation scheme based on the recent lab experimental data.

Some basic evaluations have been performed as part of the development cycle, and more detailed evaluations against a larger set of observational data sets will be performed within the other tasks of the work package (WP3), in particular Task 3.4.

CONTRIBUTION TO THE FOCI OBJECTIVES

This deliverable is the first of a series of reports on the Earth system model development activities in WP3. The work described in this report contributes to the project objective O4:

> “To improve and evaluate state-of-the-art global ESMs (WP3) and regional climate and atmospheric composition models (RCMs) (WP4), targeting specific critical processes with the largest uncertainties (WP6) for improving future next generation climate projections.”

Through this, it will contribute to the aims of WP8 under objective O7 to implement a global outreach on the overall improvement of chemistry-climate interaction in new CMIP7 cycle and up-to-date capability of the ESM to capture aerosols interaction in these processes.

1. INTRODUCTION

The work described in this report was aimed to advance the implementation of key processes associated with non-CO2 climate forcers in two ESMs, EC-Earth4 and EMAC. EC-Earth4 is the next version of the European consortium ESM EC-Earth, which is currently under development and being prepared for application in the Coupled Model Intercomparison Project phase 7 (CMIP7). The atmospheric general circulation model of EC-Earth4 is based on the OpenIFS model from the ECMWF. EMAC (ECHAM5/MESSy for Atmospheric Chemistry) is a multi-institutional project, which uses the Modular Earth Submodel System (MESSy) to link multi-institutional computer codes, in order to develop a comprehensive ESM, with special focus on atmospheric chemistry and its interactions with and feedbacks on the climate system. New modules providing more advanced descriptions of aerosols and atmospheric chemistry have been integrated in EC-Earth4 and EMAC within FOCI Project. Some basic evaluations have been performed as part of the development cycle, and more detailed evaluations against a larger set of observational data sets will be performed within the other tasks of the work package (WP3), in particular Task 3.4. In this report we aim to document the new model developments.

2. DESCRIPTION OF MODEL REVISIONS

2.1 EC-Earth4

EC-Earth is a global climate and Earth system model developed by a European consortium of national meteorological services, universities and other research institutes. The EC-Earth3 modelling framework used in the Coupled Model Intercomparison Project Phase 6 (CMIP6) consisted of the following components (Döscher et al., 2022):

- An atmospheric component based on the model used in the ECMWF Integration Forecasting System (IFS) cycle 36r4. This also includes the land surface model H-TESSEL.
- The NEMO-LIM3 global ocean–sea-ice model from the Nucleus for European Modelling of the Ocean (NEMO) release 3.6.
- The dynamic vegetation model LPJ-GUESS
- The atmospheric chemistry and transport model TM5
- The ocean biogeochemistry model PISCES from NEMO3.6
- The ice sheet model PISM for Greenland

Various configurations using different combinations of components were applied in different model intercomparison projects (MIPs). Most relevant for FOCI is the configuration with interactive aerosols and atmospheric chemistry, which uses an online two-way coupling between IFS and TM5 for simulating aerosols, ozone and methane and their interactions with the physical climate system. This configuration, called EC-Earth3-AerChem, is described in van Noije et al. (2021).

In recent years, several partners within the consortium have been putting efforts into the development of a new model generation called EC-Earth4, aimed at the next phase of CMIP (CMIP7). The first version of EC-Earth4, released in September 2024, is an atmosphere-ocean general circulation model (GCM) consisting of the following components:

- An atmospheric model based on OpenIFS 43r3

- The NEMO-SI3 global ocean–sea-ice model from NEMO 4.2

Several improvements and extensions are envisioned for future releases of EC-Earth4. FOCI contributes to these developments by improving the representation of non-CO_2 forcers in the atmospheric component of EC-Earth4, specifically of aerosols and chemically reactive trace gases.

Concerning the representation of aerosols, we have introduced a modal scheme based on the Hamburg Aerosol Model version 2.3 (HAM2.3; Tegen et al., 2019) and the M7 microphysical core (Vignati et al., 2004) to replace the AER bin-bulk scheme that comes with OpenIFS. This constitutes a major advancement. AER has evolved from the scheme developed by Morcrette et al. (2009), which simulates sulphate, hydrophilic and hydrophobic black carbon and organic matter, sea salt and mineral dust. Three bins are used for sea salt and dust, while the other components are simulated by a single tracer representing the total mass (or number of particles). In AER, the different aerosol components are externally mixed. The M7 scheme, on the other hand, describes sulphate, black carbon, organic matter, sea salt and mineral dust using seven lognormal modes, with internal mixing within the modes. Thus, by providing a more detailed description of aerosol size and composition, the new aerosol module enables a more accurate simulation of aerosol-radiation and aerosol-cloud interactions.

Regarding atmospheric chemistry, two configurations with different levels of complexity are foreseen: a standard configuration with a strongly simplified representation of what we think are the most essential chemical processes, and a configuration with a more explicit, interactive description of tropospheric and, optionally, stratospheric chemistry. The standard configuration will be the consortium's workhorse for the CMIP7 Fast Track; the chemistry configuration will be used for specific applications, such as the Aerosols and Chemistry Model Intercomparison Project (AerChemMIP) of CMIP7.

As in many other climate models, the simplified-chemistry configuration uses prescribed climatologies of the oxidants OH, H_2O_2, and O_3 to calculate the production of sulfate from oxidation of sulfur dioxide (SO_2) by the hydroxyl radical (OH) in the gas phase and from oxidation of total dissolved sulfur dioxide, S(IV), by dissolved hydrogen peroxide (H_2O_2) and ozone (O_3) in cloud droplets. In this configuration, the contributions from dimethyl sulfide (DMS) to the production of SO2 and sulfate are accounted for in a simplified way as in IFS-AER (Rémy et al., 2019). Similarly, the production of secondary organic aerosols (SOA) is accounted for following a simplified approach by enhancing the primary emissions of organic aerosols (OA).

The interactive-chemistry configuration of EC-Earth4 makes use of the tropospheric and stratospheric chemistry schemes from the IFS-COMPO model developed within the Copernicus Atmosphere Monitoring Service (CAMS). The atmospheric chemistry modules from IFS-COMPO have recently been integrated in OpenIFS 43r3 (Huijnen et al., 2022), together with the AER aerosol scheme.

Building upon this development, FMI started efforts to introduce a new, modal aerosol module based on HAM-M7 in OpenIFS 43r3. This work was continued within FOCI (Task 3.1). Meanwhile, a new version of OpenIFS based on IFS cycle 48r1 was released in January 2024. This release includes the CAMS chemistry and aerosol modules as implemented in the corresponding IFS-COMPO cycle, i.e. 48r1, by default. The EC-Earth consortium is currently working on upgrading the atmospheric component of EC-Earth4 to OpenIFS 48r1. The re-integration of the HAM-M7 based aerosol module in OpenIFS 48r1 started shortly before the official release of the new OpenIFS version and is now nearing completion. This work has been carried out as part of Task 3.1.

In the following subsections we document some of the main aspects of the new aerosol module.

2.1.1 Microphysical core

The microphysical core of HAM is based on M7 (Vignati et al., 2004). It describes sulphate (SO4), black carbon (BC), organic aerosols (OA), sea salt and mineral dust using four water-soluble modes and three water-insoluble modes in different size ranges. In terms of dry particle diameters, the size ranges considered are 0–10 nm (nucleation mode), 10–100 nm (Aitken mode), 0.1–1 µm (accumulation mode) and >1 µm (coarse mode). The nucleation mode only exists for soluble particles.

The particle size distribution in each mode is assumed to be a lognormal distribution with a fixed geometric standard deviation and variable geometric mean (median). The prognostic variables are the number of particle and the mass of the components contained in each mode.

The microphysical processes considered in M7 are nucleation, coagulation, sulfuric acid condensation and water uptake. Details on how these processes are described in M7 are given in Vignati et al. (2004). The new particle formation scheme of M7 has been modified following the approach of Bergman et al. (2022), introduced in TM5 and EC-Earth3-AerChem. This approach combines the parameterization from Vehkamäki et al. (2002) for binary homogeneous water–sulfuric acid nucleation with a semi-empirical parameterization that produces enhanced nucleation rates in the presence of low-volatility oxidized organic vapours (Riccobono et al., 2014). Other aerosol processes including emission, formation in the atmosphere, activation and cloud droplet formation, wet scavenging by clouds and precipitation, sedimentation and dry deposition, and heterogeneous chemistry on aerosol surfaces are not considered in M7. In the next subsections we briefly describe how these processes are represented in the new aerosol module.

2.1.2 Secondary organic aerosols

OpenIFS 48r1 provides an improved description of SOA production when using the AER scheme coupled to chemistry. The parameterization is taken from IFS-COMPO and describes SOA formation from biogenic, anthropogenic and biomass burning sources (ECWMF, 2023).

Biogenic SOA is produced from isoprene and monoterpenes, both of which are oxidized by OH and O_3 to form an intermediate, low-volatility gaseous precursor, which subsequently condenses to the particle phase. To account for SOA production from anthropogenic sources and biomass burning, a simplified aromatic chemistry mechanism has been introduced that describes the oxidation of toluene and xylenes by OH and O_3 to form two intermediate gaseous precursors of high and low volatility, respectively. The high-volatility precursor ages and is converted to the low-volatility precursor by reaction with OH. As for biogenic SOA, the low-volatility precursor condenses to form “anthropogenic” SOA. We have verified that this SOA production scheme is made available for use in the interactive-chemistry configuration of EC-Earth4.

To couple the SOA production to the new M7 module, five new tracers representing the SOA mass in each of the water-soluble modes and in the Aitken insoluble mode, have been added to M7. The distribution of the produced SOA mass over the different modes is calculated following Bergman et al. (2022).

As an alternative to the mechanism described above, the TM5 SOA production scheme used in EC-Earth3-AerChem has also been introduced. It describes SOA production from the oxidation of isoprene and monoterpenes by OH and O_3, using two intermediate gaseous precursors representing semi-volatile and extremely low-volatility organic compounds (Bergman et al., 2022). The partitioning of SOA precursors from gas phase to particle phase is assumed an irreversible process and thus condensed low-volatile and semi-volatile organics are combined in the particle phase SOA. This scheme is currently being coupled with the chemistry module.

2.1.3 Aerosol removal processes

In EC-Earth3-AerChem (van Noije et al., 2021), scavenging of aerosols by precipitation formation in convective and stratiform clouds is described using prescribed mode-dependent scavenging fractions for convective and stratiform clouds, while below-cloud scavenging of aerosols by stratiform precipitation is described using prescribed scavenging coefficients for the particle number and mass in each mode, estimated from results presented by Croft et al. (2009).

The HAM-M7 module implemented in OpenIFS provides an improved description of aerosol wet removal. It describes size-dependent in-cloud nucleation and impaction scavenging following the approach of Croft et al. (2010) as well as size-dependent below-cloud scavenging by rain and snow following Croft et al. (2009). The in-cloud scavenging scheme distinguishes between stratiform and convective clouds and warm, cold and mixed-phase clouds.

The calculation of aerosol dry deposition and sedimentation in OpenIFS has also been updated following the HAM implementation. Dry deposition is described using a standard resistance approach, where the deposition velocity is determined by the aerodynamic and surface resistances calculated for different surface types following Zhang et al. (2012). The surface resistances depend on the size and density of the particles. In the model, the size dependence is accounted for by using the surface resistance values at the mode number median and mass mean diameter for deposition of particle number and mass, respectively. The dry deposition calculation is described in detail in a Technical Note by Kerkweg et al. (2006). The calculation of dry deposition velocities in EC-Earth3-AerChem follows a similar approach, but with the size dependence explicitly resolved using 22 size bins over the whole size range (Aan de Brugh et al., 2011).

Sedimentation is applied to particles in the accumulation and coarse modes only. Settling velocities for particle number and mass are calculated following Zhang et al. (2012). The M7 sedimentation scheme implemented in OpenIFS provides the option to switch between an explicit and an implicit solver. The current default is to use the implicit solver of IFS-AER (Rémy et al., 2019).

2.1.4 Emissions

The OpenIFS/AC emissions pre-processing software has been adapted for use with M7. For each emission sector the specified bulk mass emissions for each component are distributed over the relevant modes and, for each of those modes, the corresponding particle number emissions are calculated based on an assumed mean or median particle diameter. The software can digest various emission inventories. Besides the CAMS emissions used in the AER and COMPO configurations of the IFS, this includes CMIP emissions. At the moment the system has been prepared to run with monthly varying historical emissions from CMIP6, i.e., anthropogenic emissions from the Community Emissions Data System (CEDS; Hoesly et al., 2018) and open biomass burning emissions from BB4CMIP (van Marle et al., 2017). In the coming months, the new CMIP7 historical and future scenario emissions will be added.

Emissions of sea salt and mineral dust are calculated online. Two distinct emission routines are available for calculating the emissions of sea salt, based on either TM5 or HAM. Both provide different options to describe the size distribution and dependence on wind speed and sea surface temperature (SST). For our purposes, we select a parameterization based on Gong (2003) but with an additional SST dependence. In the TM5 based routine, an SST dependence based on Salter et al. (2015) is adopted (Noije et al., 2021). In the HAM based routine, the temperature dependence is taken from Sofiev et al. (2011). We note that a bug was found in the HAM code in one of the expressions used to define the size distribution.

Work has been conducted in the framework of OpenIFS 48r1 to improve the representation of mineral dust. The original online dust emission scheme available in OpenIFS 48r1 is based on the AER module (Remy et al., 2019). This dust scheme follows an empirical approach and considers a dust-source dependent calibration, which is suited for forecasting operations. However, it has low sensitivity to climate-dependent variables (e.g., changes in vegetation cover, etc.) which are relevant at longer time scales. Within this task, we have worked to implement the dust emission scheme by Tegen et al. (2002), with the vegetation adjustments in Tegen et al. (2004). In this module, dust emission occurs from bare surfaces when the surface wind exceeds a certain threshold velocity, which depends on the soil particle size distribution and soil conditions. Factors like vegetation type, varying vegetation cover or snow cover modulate the source area and strength of the dust emission. The first implementation approach includes the introduction of climatological fields for some of the inputs needed by the dust scheme, including monthly varying roughness length (z), fraction of photosynthetically active radiation (FPAR), and static datasets (e.g., the potential sources of dust emission). These fields are taken from the EC-Earth3-AerChem input data to have a consistent baseline, and they could be connected online to other EC-Earth4 components in further development iterations. An evaluation of the modelled dust fields, surface concentration, deposition and dust optical depth at 550nm, including one annual cycle, will be conducted for the baseline model and the newly developed dust module.

In parallel, background work on the mineralogy datasets to be implemented within the dust emission scheme has been conducted. An implementation of 8 and 12 minerals based on the soil mineralogy maps of Claquin et al. (1999) and Journet et al. (2014) has been conducted in the EC-Earth3-AerChem and will be used as a baseline to assess the new implementation within EC-Earth4. Furthermore, analysis and evaluations of the mineral-dependent dust optical properties and ice nucleation are being conducted, building on expertise from previous projects (e.g., the ERC project FRAGMENT; https://doi.org/10.3030/773051). The knowledge gathered here will guide the subsequent steps in the EC-Earth4 developments related to Tasks 3.2 and 3.3, and the evaluation framework will be used in Task 3.4.

2.1.5 Aerosol optical and longwave radiative properties

As part of the integration of the HAM-M7 modal aerosol module in OpenIFS, aerosols have been coupled to the radiation scheme through their optical properties. These properties include the extinction cross section, single-scattering albedo, and asymmetry factor, each calculated for the specific wavelengths used in the radiation scheme. There are two options for calculating these optical properties: the TM5 scheme from EC-Earth3-AerChem and a new scheme from HAM-M7, with the latter now set as the default. Both schemes compute optical properties for 14 shortwave wavelength bands. The new HAM-M7 scheme also calculates these properties for 16 longwave wavelengths. However, only the extinction cross section for longwave radiation wavelengths is passed to the radiation module, with the single-scattering albedo set to 0. Thus, aerosols are considered fully absorbing at these longwave wavelengths.

The model dynamically computes the radiative properties of aerosols by deriving the Mie scattering size parameter and volume-averaged refractive indices from the chemical composition, including water content, and particle size of each mode. It assumes internal mixing of the different chemical components within the modes. These parameters are then put into a lookup table, which provides the extinction cross section, single-scattering albedo, and asymmetry parameter. This lookup table is constructed using Mie theory and accommodates 14 spectral bands for shortwave radiation and 16 bands for longwave radiation used by the radiative scheme. The refractive indices of different aerosol species are listed in Zhang et al. (2012).

Modal schemes like M7 have difficulty in accurately representing both tropospheric and stratospheric aerosols using the same modal setup, as noted by Kokkola et al. (2009). To address this for CMIP6 simulations using EC-Earth3-AerChem, a solution was adopted that combines aerosol optical properties from the M7 modal scheme for the troposphere with prescribed CMIP6 optical properties for stratospheric aerosols. This approach has now been implemented in OpenIFS 48r1 as well. In this method, the prescribed stratospheric aerosol optical properties are read from 4-dimensional netCDF files and used alongside the simulated aerosol optical properties from HAM-M7. For CMIP7 simulations, a similar set of stratospheric optical properties will be made available.

2.1.6 Activation scheme

Activation of aerosols to form cloud droplets is not explicitly represented in the IFS. As part of the integration of the new modal aerosol module, the activation scheme from Abdul-Razzak and Ghan (2000) has been introduced in OpenIFS. The implementation of this scheme follows that in EC-Earth3, including the treatment of the updraft vertical velocity and the way the cloud droplet number concentrations calculated in the activation scheme are coupled to the radiation scheme and the cloud microphysics (Döscher et al., 2022; van Noije et al., 2021). Meanwhile, an improved parameterization of droplet activation based on the work of Morales Betancourt and Nenes (2014) and a parameterization of the updraft velocity depending on turbulent kinetic energy (TKE), have been introduced in OpenIFS. This work builds on post-CMIP6 developments of EC-Earth3 from the FORCeS project, described in a recent publication by Thomas et al. (2024), and is carried out in collaboration with the Horizon Europe project CleanCloud (https://doi.org/10.3030/101137639). More details on these developments will be provided in Deliverable 3.3.

2.1.7 Summary of the improvements compared to EC-Earth3-AerChem

The use of a single atmospheric model component with integrated modules for atmospheric chemistry and aerosols in EC-Earth4 supersedes the use of TM5 and 6-hourly data exchange between TM5 and IFS in EC-Earth3-AerChem. This improves both the consistency of the simulation and the computational efficiency of the model. At the same time, it is currently not possible to run chemistry and aerosols at a lower spatial resolution than the dynamics and physics of the general circulation model, as is done in EC-Earth3-AerChem.

In addition to the upgrade from IFS 36r4 to OpenIFS 48r1, which by itself constitutes a major improvement in terms of the representation of the general circulation, the development activities outlined above have improved the treatment of multiple physico-chemical processes compared to how these were described in TM5. The most noteworthy improvements are: an updated description of aerosol wet scavenging, both in and below clouds, which is now fully consistent with the original work by Croft et al. (2009) and Croft et al. (2010); a more direct computation of longwave radiative properties of tropospheric aerosols; the introduction of an improved activation scheme (Morales Betancourt and Nenes, 2014) with TKE dependent updraft velocity; an updated tropospheric chemical mechanism (Williams et al., 2022; Eskes et al., 2024) and the addition of a comprehensive stratospheric chemistry scheme (Huijnen et al., 2016; Eskes et al., 2024).

2.2 EMAC

The EMAC (ECHAM/MESSy Atmospheric Chemistry) model is an ESM incorporating various sub-models for simulating coupled atmosphere-ocean-land system and anthropogenic aspects using the second version of the Modular Earth Submodel System (MESSy2) interface, which is a multi-institutional development effort (Jöckel et al., 2006; 2010). The atmospheric dynamics core of EMAC is the 5th generation European Centre Hamburg general circulation model (ECHAM5; Roeckner et al., 2003). The physics subroutines of the original ECHAM5 code have been reimplemented as MESSy submodels and have continuously been further developed. The spectral transform core, the flux-form semi-Lagrangian large-scale advection scheme and the atmospheric relaxation towards the observed state (nudging; Jeuken et al., 1996) routines remain within the ECHAM5 core. The simulations within FOCI typically use the T63L31 resolution, which corresponds to a horizontal model grid spacing of 1.875° (approx. 200 km at the equator) with 31 vertical hybrid-sigma-pressure levels up to 10 hPa (about 31 km) altitude. Model dynamics are nudged towards the fifth generation of the European Centre for Medium-Range Weather Forecasts (ECMWF) reanalysis data (ERA5; Hersbach et al., 2020). Relevant long-lived trace gases (CO_2, CH_4, N_2O, chlorofluorocarbons (CFCs), hydrochlorofluorocarbons (HCFCs), halons and

H_2) are conventionally assimilated (tracer-nudged) towards observed surface values. Furthermore, EMAC employs the following sub-models relevant to the atmospheric constituents' physico-chemical representation:

- Comprehensive atmospheric gas-phase kinetics: MECCA v4.2 (Sander et al., 2019)
- Comprehensive aerosol physics and chemistry: GMXe v2.2.1 (Pringle et al., 2010)
- Formation of secondary organic aerosol (SOA) via condensation of semi-, intermediate-volatile and volatile organic compounds (S-/I-/VOCs): ORACLE v1.2 (Tsimpidi et al., 2014)
- New aerosol particle formation rates calculation for ion-induced and pure organic species: NAN v1.1/IONS v1.0 (Ehrhart et al., 2018)
- Other gas-phase and aerosol emission and removal processes: dry deposition (DRYDEP), wet scavenging (SCAV) and sedimentation (SEDI), off-line (prescribed) and on-line (parameter-driven) emissions (OFFEMIS) (Jöckel et al., 2016)

In the following, we describe the developments accomplished within the project deliverable D3.1 aimed at the improved EMAC representation of tropospheric sulphate formation. These include (1) implementation of comprehensive kinetic chemistry of sulfuric acid formation from natural precursors such as dimethyl sulfate (DMS, CH_3SO_2) and relevant intermediates such as methane sulfonic acid (MSA, CH_3SO_3H), and (2) implementation of the new particle formation scheme based on the recent lab experimental data.

2.2.1 Implementation of novel DMS gas-phase oxidation mechanisms in EMAC

The chemical kinetics scheme (mechanism) used in EMAC/MECCA is an extended and updated version of the Mainz Isoprene Mechanism (MIM) comprising 176 gas-phase tracers in over 390 (297 gas-phase, 82 photolysis and 12 heterogeneous) reactions. The detailed description of MIM can be found in the Supplement to Jöckel et al. (2016). The new development concerns the extension of the DMS oxidation part of MIM which originally contained 11 gas-phase reactions of DMS and a limited set of its oxidation products. The oxidation pathways are governed by the hydroxyl radical (OH); other pathways include reactions with halogen monoxides (BrO, IO), abstraction pathways via nitrate radical (NO_3), chlorine- and bromine-initiated reactions with DMS. The products and major intermediates include the hydrocarboxyl radical (HCOC), sulphur dioxide (SO_2), and MSA. The latter in MIM is solely produced through the oxidation of DMS by ozone (O_3) and the hydroperoxyl radical (HO_2), with CH_3SO_2 being the intermediate product of the DMS abstraction pathway.

Earlier validations of the MIM DMS oxidation mechanism revealed consistent overestimation of gas-phase MSA compared to observed values, likely resulting from oversimplified representation of MSA gas-phase kinetics. Within the deliverable D3.1, the first objective is focused on improvement of the organic sulphur gas-phase kinetics, viz. introduction of alternative DMS oxidation schemes in EMAC based on the mechanisms proposed by Fung et al. (2022) ("FU22" hereafter), Shen et al. (2022) ("SH22") and the respective subset of the Master Chemical Mechanism ("MCM"; Saunders et al., 2003). We refer to the cited literature for the details on each mechanism implementation which are omitted here for terseness. A noteworthy advantage of the implemented schemes is the inclusion of the hydroperoxymethyl thioformate (HPMTF, CH_3SO_2CHO) otherwise not present in MIM. Recent studies indicate that HPMTF is an intermediate with significantly long lifetime that contains up to 30% of the DMS-derived sulphur in the troposphere (e.g., Veres et al., 2020).

A preliminary validation of each scheme was performed against the observational data on gas-phase and aerosol physico-chemical properties collected in the Arctic Ocean (MOCCHA campaign, August–September 2018; Leck et al., 2019) and Southern Ocean (Arctic Circumnavigation Expedition, December 2016–March 2017; Landwehr et al., 2021). The results indicate a substantial improvement of the MSA abundances in two of the four evaluated mechanisms (see Fig. 1). In these simulations, EMAC terrestrial DMS emissions are based on inventories by Spiro et al. (1992), whereas the oceanic DMS fluxes are calculated using the AIRSEA submodel

(Pozzer et al., 2006) in combination with the ocean surface concentrations climatology (Hulswar et al., 2022). The resulting oceanic DMS emission is 7–11% higher compared to the recent estimates (Hulswar et al., 2022; Lana et al., 2011), which is in a very good agreement compared to an order of magnitude or larger discrepancies typically resulting from underestimation of sea ice ratio, differences in the land-sea masks or inadequately simulated air-sea exchange fluxes. We conclude that the newly introduced FU22 and SH22 schemes in EMAC allow for more accurate study of MSA-induced SOA formation.

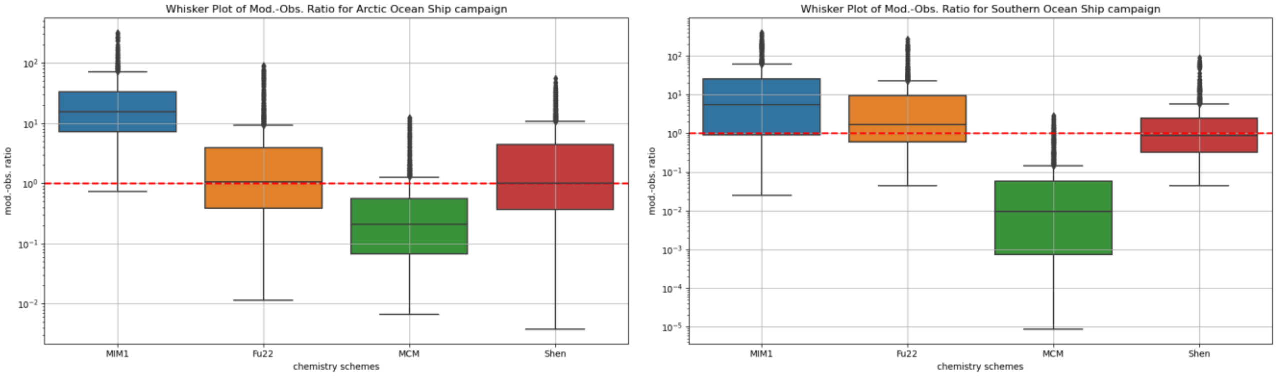

Figure 1. Statistics (box-whisker plots) of the model-to-observation ratio of MSA simulated in EMAC in the Arctic Ocean (left) and Southern Ocean (right). The best-fitting result is obtained at the 1:1 ratio indicated with the red dotted line; mind the vertical logarithmic scale. Colours denote to various DMS-MSA kinetic mechanisms used: MIM (blue), FU22 (yellow), MCM (green) and SH22 (red). Box/whiskers refer to 25–75 percentiles/1.5 IQR ranges of the distributions, respectively.

2.2.2 New aerosol particle formation scheme implementation

A second objective of the deliverable D3.1 consists of the extension of the new particle formation (NPF) rates parameterisation schemes available in EMAC. The novel mechanism of SOA formation involving MSA has been implemented following the recent NPF experimental data from the CLOUD (Cosmics Leaving OUtdoor Droplets; Dada et al., 2024) chamber experiments at CERN. In brief, DMS oxidation proceeds via multiple precursors leading to formation of sulfuric acid (SA, H_2SO_4) and MSA. Whilst NPF promoted by the former is recognised and implemented in ESMs, the experimental evidence for MSA-driven nucleation was recently established and kinetics were quantified in CLOUD experiments (Baalbaki et al., in prep.). The proposed mechanism of MSA-driven NPF (Dunne et al., 2016; Hodshire et al., 2019) assumes two nucleating regimes, namely (1) neutral, SA-like nucleation rate at MSA abundances not exceeding a given threshold level, and (2) ion-induced ternary nucleation in presence of ammonia (NH_3) and/or cosmic ray ions. Such MSA NPF parameterisation was implemented in EMAC (submodels NAN coupled with submodel IONS) and assessed with the EMAC-reproduced NH_3, water vapour and MSA abundances available from the four DMS/MSA oxidation mechanisms.

The preliminary comparison of EMAC particle concentrations in the marine boundary layer (MBL) and free troposphere against observational data (particle density profiles available from the ATom campaigns; Brock et al., 2019) indicates the best-fitting DMS/MSA kinetics for the new MSA NPF is the newly implemented SH22 mechanism, with most robust results obtained within the MBL. A detailed evaluation with EMAC (including longer simulation periods and other observational campaigns) is to follow. From the preliminary evaluation simulations we have obtained the first estimates of the MSA-related nucleation radiative forcing (RF, instantaneous). On a global scale, MSA NPF-induced RF amounts to $-0.74\mathrm{W/m^2}$ (indirect, cloud-aerosol interaction) and $-0.11\ \mathrm{W/m^2}$ (direct aerosol scattering effect), which strongly impacts radiative balance particularly over the Southern Ocean region (see Fig. 2). We note that large spatial fluctuations in RF response are obtained due to the relatively short time span of the preliminary evaluation simulations (3 years), which will be addressed in subsequent evaluation iterations with EMAC.

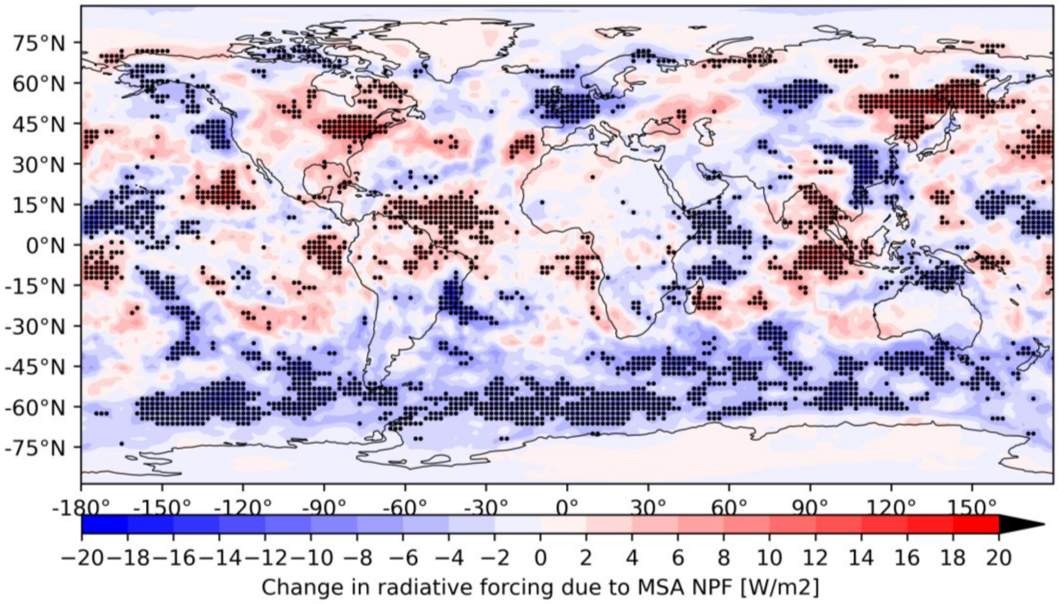

Figure 2. Change in the instantaneous radiative forcing due to the new MSA NPF with the SH22 DMS/MSA gas-phase kinetics implemented in EMAC (see text for details). Shown is the annual average from a preliminary 3-year long simulation. Dotted areas denote statistically significant results (CI of 95%, two-sided test).

3. OUTLOOK

We have reported on advancements made in the representation of aerosols and atmospheric chemistry in EC-Earth4 and EMAC. Details on developments related to aerosol radiative properties and aerosol-cloud interactions will be given in Deliverables D3.2 and D3.3, respectively.

The OpenIFS developments documented in this report exploit and strengthen interactions with the atmospheric chemistry modelling activities undertaken in the CAMS programme. Efforts to introduce the new modal aerosol module into IFS-COMPO 49r1 are currently undertaken in the Horizon Europe project CAMAERA (https://camaera-project.eu/). In this way, the work reported here paves the way for advancing the representation of aerosols and their interactions with radiation and clouds in the CAMS operational system.

For EMAC, we have presented results on the impacts of a novel DMS oxidation mechanism and new particle formation scheme. In the coming months a large part of the efforts in WP3 will be devoted to evaluation of the models' performance using both existing observational data sets and new data sets compiled within the project. Results of the evaluation analyses will be reported in D3.4.

4. REFERENCES

Abdul-Razzak, H. and Ghan, S. J.: A parameterization of aerosol activation: 2. Multiple aerosol types, J. Geophys. Res., 105, 6837–6844, https://doi.org/10.1029/1999JD901161, 2000.

Bergman, T., Makkonen, R., Schrödner, R., Swietlicki, E., Phillips, V. T. J., Le Sager, P., and van Noije, T.: Description and evaluation of a secondary organic aerosol and new particle formation scheme within TM5-MP v1.2, Geosci. Model Dev., 15, 683–713, https://doi.org/10.5194/gmd-15-683-2022, 2022.

Brock, C. A., Williamson, C., Kupc, A., Froyd, K. D., Erdesz, F., Wagner, N., Richardson, M., Schwarz, J. P., Gao, R.-S., Katich, J. M., Campuzano-Jost, P., Nault, B. A., Schroder, J. C., Jimenez, J. L., Weinzierl, B., Dollner, M., Bui, T., and Murphy, D. M.: Aerosol size distributions during the atmospheric tomography mission (ATom): methods, uncertainties, and data products, Atmos. Meas. Tech., 12, 3081–3099, https://doi.org/10.5194/amt-12-3081-2019, 2019.

Claquin, T., Schulz, M., and Balkanski, Y. J.: Modeling the mineralogy of atmospheric dust sources, J. Geophys. Res., 104(D18), 22243–22256, https://doi.org/10.1029/1999JD900416, 1999.

Croft, B., Lohmann, U., Martin, R. V., Stier, P., Wurzler, S., Feichter, J., Posselt, R., and Ferrachat, S.: Aerosol size-dependent below-cloud scavenging by rain and snow in the ECHAM5-HAM, Atmos. Chem. Phys., 9, 4653–4675, https://doi.org/10.5194/acp-9-4653-2009, 2009.

Croft, B., Lohmann, U., Martin, R. V., Stier, P., Wurzler, S., Feichter, J., Hoose, C., Heikkilä, U., van Donkelaar, A., and Ferrachat, S.: Influences of in-cloud aerosol scavenging parameterizations on aerosol concentrations and wet deposition in ECHAM5-HAM, Atmos. Chem. Phys., 10, 1511–1543, https://doi.org/10.5194/acp-10-1511-2010, 2010.

Dada, L., Huang, W., and El-Haddad, I.: Molecular mechanisms of aerosol nucleation: from CLOUD chamber experiments to field observations, Chimia, 78, 739–747, https://doi.org/10.2533/chimia.2024.739, 2024.

Döscher, R., Acosta, M., Alessandri, A., Anthoni, P., Arsouze, T., Bergman, T., Bernardello, R., Boussetta, S., Caron, L.-P., Carver, G., Castrillo, M., Catalano, F., Cvijanovic, I., Davini, P., Dekker, E., Doblas-Reyes, F. J., Docquier, D., Echevarria, P., Fladrich, U., Fuentes-Franco, R., Gröger, M., v. Hardenberg, J., Hieronymus, J., Karami, M. P., Keskinen, J.-P., Koenigk, T., Makkonen, R., Massonnet, F., Ménégoz, M., Miller, P. A., Moreno-Chamarro, E., Nieradzik, L., van Noije, T., Nolan, P., O'Donnell, D., Ollinaho, P., van den Oord, G., Ortega, P., Prims, O. T., Ramos, A., Reerink, T., Rousset, C., Ruprich-Robert, Y., Le Sager, P., Schmith, T., Schrödner, R., Serva, F., Sicardi, V., Sloth Madsen, M., Smith, B., Tian, T., Tourigny, E., Uotila, P., Vancoppenolle, M., Wang, S., Wårlind, D., Willén, U., Wyser, K., Yang, S., Yepes-Arbós, X., and Zhang, Q.: The EC-Earth3 Earth system model for the Coupled Model Intercomparison Project 6, Geosci. Model Dev., 15, 2973–3020, https://doi.org/10.5194/gmd-15-2973-2022, 2022.

Dunne, E. M., Gordon, H., Kürten, A., Almeida, J., Duplissy, J., Williamson, C., Ortega, I. K., Pringle, K. J., Adamov, A., Baltensperger, U., Barmet, P., Benduhn, F., Bianchi, F., Breitenlechner, M., Clarke, A., Curtius, J., Dommen, J., Donahue, N. M., Ehrhart, S., Flagan, R. C., Franchin, A., Guida, R., Hakala, J., Hansel, A., Heinritzi, M., Jokinen, T., Kangasluoma, J., Kirkby, J., Kulmala, M., Kupc, A., Lawler, M. J., Lehtipalo, K., Makhmutov, V., Mann, G., Mathot, S., Merikanto, J., Miettinen, P., Nenes, A., Onnela, A., Rap, A., Reddington, C. L. S., Riccobono, F., Richards, N. A. D., Rissanen, M. P., Rondo, L., Sarnela, N., Schobesberger, S., Sengupta, K., Simon, M., Sipilä, M., Smith, J. N., Stozkhov, Y., Tomé, A., Tröstl, J., Wagner, P. E., Wimmer, D., Winkler, P. M., Worsnop, D. R., and Carslaw, K. S.: Global atmospheric particle formation from CERN CLOUD measurements, Science, 354, 1119–1124, https://doi.org/10.1126/science.aaf2649, 2016.

ECMWF: IFS Documentation CY48R1 – Part VIII: Atmospheric Composition, ECMWF, pp. 84, https://doi.org/10.21957/749dc09059, 2023.

Ehrhart, S., Dunne, E. M., Manninen, H. E., Nieminen, T., Lelieveld, J., and Pozzer, A.: Two new submodels for the modular earth submodel system (MESSy): new aerosol nucleation (NAN) and small ions (IONS) version 1.0, Geosci. Model Dev., 11, 4987–5001, https://doi.org/10.5194/gmd-11-4987-2018, 2018.

Eskes, H., Tsikerdekis, A., Ades, M., Alexe, M., Benedictow, A. C., Bennouna, Y., Blake, L., Bouarar, I., Chabrillat, S., Engelen, R., Errera, Q., Flemming, J., Garrigues, S., Griesfeller, J., Huijnen, V., Ilić, L., Inness, A., Kapsomenakis, J., Kipling, Z., Langerock, B., Mortier, A., Parrington, M., Pison, I., Pitkänen, M., Remy, S., Richter, A., Schoenhardt, A., Schulz, M., Thouret, V., Warneke, T., Zerefos, C., and Peuch, V.-H.: Technical note: Evaluation of the Copernicus Atmosphere Monitoring Service Cy48R1 upgrade of June 2023, Atmos. Chem. Phys., 24, 9475–9514, https://doi.org/10.5194/acp-24-9475-2024, 2024.

Fung, K. M., Heald, C. L., Kroll, J. H., Wang, S., Jo, D. S., Gettelman, A., Lu, Z., Liu, X., Zaveri, R. A., Apel, E. C., Blake, D. R., Jimenez, J.-L., Campuzano-Jost, P., Veres, P. R., Bates, T. S., Shilling, J. E., and Zawadowicz, M.: Exploring dimethyl sulfide (DMS) oxidation and implications for global aerosol radiative forcing, Atmos. Chem. Phys., 22, 1549–1573, https://doi.org/10.5194/acp-22-1549-2022, 2022.

Gong, S. L.: A parameterization of sea-salt aerosol source function for sub- and super-micron particles, Global Biogeochem. Cy., 17, 1097, https://doi.org/10.1029/2003GB002079, 2003.

Hersbach, H., Bell, B., Berrisford, P., Hirahara, S., Horányi, A., Muñoz-Sabater, J., Nicolas, J., Peubey, C., Radu, R., Schepers, D., Simmons, A., Soci, C., Abdalla, S., Abellan, X., Balsamo, G., Bechtold, P., Biavati, G., Bidlot, J., Bonavita, M., De Chiara, G., Dahlgren, P., Dee, D., Diamantakis, M., Dragani, R., Flemming, J., Forbes, R., Fuentes, M., Geer, A., Haimberger, L., Healy, S., Hogan, R. J., Hólm, E., Janisková, M., Keeley, S., Laloyaux, P., Lopez, P., Lupu, C., Radnoti, G., de Rosnay, P., Rozum, I., Vamborg, F., Villaume, S., and Thépaut, J.-N.: The ERA5 global reanalysis, Q. J. R. Meteorolog. Soc., 146, 1999–2049, https://doi.org/10.1002/qj.3803, 2020.

Hodshire, A. L., Campuzano-Jost, P., Kodros, J. K., Croft, B., Nault, B. A., Schroder, J. C., Jimenez, J. L., and Pierce, J. R.: The potential role of methanesulfonic acid (MSA) in aerosol formation and growth and the associated radiative forcings, Atmos. Chem. Phys., 19, 3137–3160, https://doi.org/10.5194/acp-19-3137-2019, 2019.

Hoesly, R. M., Smith, S. J., Feng, L., Klimont, Z., Janssens-Maenhout, G., Pitkanen, T., Seibert, J. J., Vu, L., Andres, R. J., Bolt, R. M., Bond, T. C., Dawidowski, L., Kholod, N., Kurokawa, J.-I., Li, M., Liu, L., Lu, Z., Moura, M. C. P., O'Rourke, P. R., and Zhang, Q.: Historical (1750–2014) anthropogenic emissions of reactive gases and aerosols from the Community Emissions Data System (CEDS), Geosci. Model Dev., 11, 369–408, https://doi.org/10.5194/gmd-11-369-2018, 2018.

Huijnen, V., Flemming, J., Chabrillat, S., Errera, Q., Christophe, Y., Blechschmidt, A.-M., Richter, A., and Eskes, H.: C-IFS-CB05-BASCOE: stratospheric chemistry in the Integrated Forecasting System of ECMWF, Geosci. Model Dev., 9, 3071–3091, https://doi.org/10.5194/gmd-9-3071-2016, 2016.

Huijnen, V., Le Sager, P., Köhler, M. O., Carver, G., Rémy, S., Flemming, J., Chabrillat, S., Errera, Q., and van Noije, T.: OpenIFS/AC: atmospheric chemistry and aerosol in OpenIFS 43r3, Geosci. Model Dev., 15, 6221–6241, https://doi.org/10.5194/gmd-15-6221-2022, 2022.

Hulswar, S., Simó, R., Galí, M., Bell, T. G., Lana, A., Inamdar, S., Halloran, P. R., Manville, G., and Mahajan, A. S.: Third revision of the global surface seawater dimethyl sulfide climatology (DMS-Rev3), Earth Syst. Sci. Data, 14, 2963–2987, https://doi.org/10.5194/essd-14-2963-2022, 2022.

Jeuken, A. B. M., Siegmund, P. C., Heijboer, L. C., Feichter, J., and Bengtsson, L.: On the potential of assimilating meteorological analyses in a global climate model for the purpose of model validation, J. Geophys. Res.: Atmos., 101, 16939−16950, https://doi.org/10.1029/96jd01218, 1996.

Jöckel, P., Tost, H., Pozzer, A., Brühl, C., Buchholz, J., Ganzeveld, L., Hoor, P., Kerkweg, A., Lawrence, M. G., Sander, R., Steil, B., Stiller, G., Tanarhte, M., Taraborrelli, D., van Aardenne, J., and Lelieveld, J.: The atmospheric chemistry general circulation model ECHAM5/MESSy1: consistent simulation of ozone from the surface to the mesosphere, Atmos. Chem. Phys., 6, 5067−5104, https://doi.org/10.5194/acp-6-5067-2006, 2006.

Jöckel, P., Kerkweg, A., Pozzer, A., Sander, R., Tost, H., Riede, H., Baumgaertner, A., Gromov, S., and Kern, B.: Development cycle 2 of the modular earth submodel system (MESSy2), Geosci. Model Dev., 3, 717−752, https://doi.org/10.5194/gmd-3-717-2010, 2010.

Jöckel, P., Tost, H., Pozzer, A., Kunze, M., Kirner, O., Brenninkmeijer, C. A. M., Brinkop, S., Cai, D. S., Dyroff, C., Eckstein, J., Frank, F., Garny, H., Gottschaldt, K.-D., Graf, P., Grewe, V., Kerkweg, A., Kern, B., Matthes, S., Mertens, M., Meul, S., Neumaier, M., Nützel, M., Oberländer-Hayn, S., Ruhnke, R., Runde, T., Sander, R., Scharffe, D., and Zahn, A.: Earth system chemistry integrated modelling (ESCiMo) with the modular earth submodel system (MESSy) version 2.51, Geosci. Model Dev., 9, 1153–1200, https://doi.org/10.5194/gmd-9-1153-2016, 2016.

Journet, E., Balkanski, Y., and Harrison, S. P.: A new data set of soil mineralogy for dust-cycle modeling, Atmos. Chem. Phys., 14, 3801–3816, https://doi.org/10.5194/acp-14-3801-2014, 2014.

Kerkweg, A., Buchholz, J., Ganzeveld, L., Pozzer, A., Tost, H., and Jöckel, P.: Technical Note: An implementation of the dry removal processes DRY DEPosition and SEDImentation in the Modular Earth Submodel System (MESSy), Atmos. Chem. Phys., 6, 4617–4632, https://doi.org/10.5194/acp-6-4617-2006, 2006.

Kokkola, H., Hommel, R., Kazil, J., Niemeier, U., Partanen, A.-I., Feichter, J., and Timmreck, C.: Aerosol microphysics modules in the framework of the ECHAM5 climate model – intercomparison under stratospheric conditions, Geosci. Model Dev., 2, 97–112, https://doi.org/10.5194/gmd-2-97-2009, 2009.

Lana, A., Bell, T. G., Simó, R., Vallina, S. M., Ballabrera-Poy, J., Kettle, A. J., Dachs, J., Bopp, L., Saltzman, E. S., Stefels, J., Johnson, J. E., and Liss, P. S.: An updated climatology of surface dimethlysulfide concentrations and emission fluxes in the global ocean, Global Biogeochem. Cycles, 25, https://doi.org/10.1029/2010GB003850, 2011.

Landwehr, S., Volpi, M., Haumann, F. A., Robinson, C. M., Thurnherr, I., Ferracci, V., Baccarini, A., Thomas, J., Gorodetskaya, I., Tatzelt, C., Henning, S., Modini, R. L., Forrer, H. J., Lin, Y., Cassar, N., Simó, R., Hassler, C., Moallemi, A., Fawcett, S. E., Harris, N., Airs, R., Derkani, M. H., Alberello, A., Toffoli, A., Chen, G., Rodríguez-Ros, P., Zamanillo, M., Cortés-Greus, P., Xue, L., Bolas, C. G., Leonard, K. C., Perez-Cruz, F., Walton, D., and Schmale, J.: Exploring the coupled ocean and atmosphere system with a data science approach applied to observations from the antarctic circumnavigation expedition, Earth Syst. Dyn., 12, 1295–1369, https://doi.org/10.5194/esd-12-1295-2021, 2021.

Leck, C., Matrai, P., Perttu, A.-M., and Gårdfeldt, K.: Expedition report: SWEDARTIC arctic ocean 2018, Swedish Polar Research Secretariat, 2019.

Morales Betancourt, R. and Nenes, A.: Droplet activation parameterization: the population-splitting concept revisited, Geosci. Model Dev., 7, 2345–2357, https://doi.org/10.5194/gmd-7-2345-2014, 2014.

Morcrette, J.-J., Boucher, O., Jones, L., Salmond, D., Bechtold, P., Beljaars, A., Benedetti, A., Bonet, A., Kaiser, J. W., Razinger, M., Schulz, M., Serrar, S., Simmons, A. J., Sofiev, M., Suttie, M., Tompkins, A. M., and Untch, A.: Aerosol analysis and forecast in the European Centre for Medium-Range Weather Forecasts Integrated Forecast System: Forward modeling, J. Geophys. Res., 114, D06206, doi:10.1029/2008JD011235, 2009.

Pozzer, A., Jöckel, P., Sander, R., Williams, J., Ganzeveld, L., and Lelieveld, J.: Technical note: the MESSy-submodel AIRSEA calculating the air-sea exchange of chemical species, Atmos. Chem. Phys., 6, 5435–5444, https://doi.org/10.5194/acp-6-5435-2006, 2006.

Pringle, K. J., Tost, H., Message, S., Steil, B., Giannadaki, D., Nenes, A., Fountoukis, C., Stier, P., Vignati, E., and Lelieveld, J.: Description and evaluation of GMXe: a new aerosol submodel for global simulations (v1), Geosci. Model Dev., 3, 391–412, https://doi.org/10.5194/gmd-3-391-2010, 2010.

Rémy, S., Kipling, Z., Flemming, J., Boucher, O., Nabat, P., Michou, M., Bozzo, A., Ades, M., Huijnen, V., Benedetti, A., Engelen, R., Peuch, V.-H., and Morcrette, J.-J.: Description and evaluation of the tropospheric aerosol scheme in the European Centre for Medium-Range Weather Forecasts (ECMWF) Integrated Forecasting System (IFS-AER, cycle 45R1), Geosci. Model Dev., 12, 4627–4659, https://doi.org/10.5194/gmd-12-4627-2019, 2019.

Riccobono F., Schobesberger S., Scott C. E., Dommen, J., Ortega, I. K., Rondo, L., Almeida, J., Amorim, A., Bianchi, F., Breitenlechner, M., David, A., Downard, A., Dunne, E. M., Duplissy, J., Ehrhart, S., Flagan, R. C., Franchin, A., Hansel, A., Junninen, H., Kajos, M., Keskinen, H., Kupc, A., Kürten, A., Kvashin, A. N., Laaksonen, A., Lehtipalo, K., Makhmutov, V., Mathot, S., Nieminen, T., Onnela, A., Petäjä, T., Praplan, A. P., Santos, F. D., Schallhart, S., Seinfeld, J. H., Sipilä, M., Spracklen, D. V., Stozhkov, Y., Stratmann, F., Tomé, A., Tsagkogeorgas, G., Vaattovaara, P., Viisanen, Y., Vrtala, A., Wagner, P. E., Weingartner, E., Wex, H., Wimmer, D., Carslaw, K. S., Curtius, J., Donahue, N. M., Kirkby, J., Kulmala, M., Worsnop, D. R., and Baltensperger, U.: Oxidation products of biogenic emissions contribute to nucleation of atmospheric particles, Science, 344, 717–721, https://doi.org/10.1126/science.1243527, 2014.

Roeckner, E., Bäuml, G., Bonaventura, L., Brokopf, R., Esch, M., Giorgetta, M., Hagemann, S., Kirchner, I., Kornblue, L., Manzini, E., Rhodin, A., Schleese, U., Schulzweida, U., and Tompkins, A.: The atmospheric general circulation model ECHAM5: part 1, Max-Planck-Institut für Meteorologie, 2003.

Salter, M. E., Zieger, P., Acosta Navarro, J. C., Grythe, H., Kirkevåg, A., Rosati, B., Riipinen, I., and Nilsson, E. D.: An empirically derived inorganic sea spray source function incorporating sea surface temperature, Atmos. Chem. Phys., 15, 11047–11066, https://doi.org/10.5194/acp-15-11047-2015, 2015.

Sander, R., Baumgaertner, A., Cabrera, D., Frank, F., Grooß, J. U., Gromov, S., Harder, H., Huijnen, V., Jöckel, P., Karydis, V. A., Niemeyer, K. E., Pozzer, A., Riede, H., Schultz, M. G., Taraborrelli, D., and Tauer, S.: The community atmospheric chemistry box model CAABA/MECCA-4.0, Geosci. Model Dev., 12, 1365−1385, https://doi.org/10.5194/gmd-12-1365-2019, 2019.

Saunders, S. M., Jenkin, M. E., Derwent, R. G., and Pilling, M. J.: Protocol for the development of the master chemical mechanism, MCM v3 (part a): tropospheric degradation of non-aromatic volatile organic compounds, Atmos. Chem. Phys., 3, 161−180, https://doi.org/10.5194/acp-3-161-2003, 2003.

Shen, J., Scholz, W., He, X.-C., Zhou, P., Marie, G., Wang, M., Marten, R., Surdu, M., Rörup, B., Baalbaki, R., Amorim, A., Ataei, F., Bell, D. M., Bertozzi, B., Brasseur, Z., Caudillo, L., Chen, D., Chu, B., Dada, L., Duplissy, J., Finkenzeller, H., Granzin, M., Guida, R., Heinritzi, M., Hofbauer, V., Iyer, S., Kemppainen, D., Kong, W., Krechmer, J. E., Kürten, A., Lamkaddam, H., Lee, C. P., Lopez, B., Mahfouz, N. G. A., Manninen, H. E., Massabò, D., Mauldin, R. L., Mentler, B., Müller, T., Pfeifer, J., Philippov, M., Piedehierro, A. A., Roldin, P., Schobesberger, S., Simon, M., Stolzenburg, D., Tham, Y. J., Tomé, A., Umo, N. S., Wang, D., Wang, Y., Weber, S. K., Welti, A., Wollesen de Jonge, R., Wu, Y., Zauner-Wieczorek, M., Zust, F., Baltensperger, U., Curtius, J., Flagan, R. C., Hansel, A., Möhler, O., Petäjä, T., Volkamer, R., Kulmala, M., Lehtipalo, K., Rissanen, M., Kirkby, J., El-Haddad, I., Bianchi, F., Sipilä, M., Donahue, N. M., and Worsnop, D. R.: High gas-phase methanesulfonic acid production in the OH-initiated oxidation of dimethyl sulfide at low temperatures, Environ. Sci. Technol., 56, 13931–13944, https://doi.org/10.1021/acs.est.2c05154, 2022.

Sofiev, M., Soares, J., Prank, M., de Leeuw, G., and Kukkonen, J.: A regional-to-global model of emission and transport of sea salt particles in the atmosphere, J. Geophys. Res., 116, D21302, https://doi.org/10.1029/2010JD014713, 2011.

Spiro, P. A., Jacob, D. J., and Logan, J. A.: Global inventory of sulfur emissions with 1°×1° resolution, J. Geophys. Res.: Atmos., 97, 6023–6036, https://doi.org/10.1029/91JD03139, 1992.

Tegen, I., Harrison, S. P., Kohfeld, K., Prentice, I. C., Coe, M., and Heimann, M.: Impact of vegetation and preferential source areas on global dust aerosol: Results from a model study, J. Geophys. Res., 107(D21), 4576, https://doi.org/10.1029/2001JD000963, 2002.

Tegen, I., Werner, M., Harrison, S. P., and Kohfeld, K. E.: Relative importance of climate and land use in determining present and future global soil dust emission, Geophys. Res. Lett., 31, L05105, https://doi.org/10.1029/2003GL019216, 2004.

Tegen, I., Neubauer, D., Ferrachat, S., Siegenthaler-Le Drian, C., Bey, I., Schutgens, N., Stier, P., Watson-Parris, D., Stanelle, T., Schmidt, H., Rast, S., Kokkola, H., Schultz, M., Schroeder, S., Daskalakis, N., Barthel, S., Heinold, B., and Lohmann, U.: The global aerosol–climate model ECHAM6.3–HAM2.3 – Part 1: Aerosol evaluation, Geosci. Model Dev., 12, 1643–1677, https://doi.org/10.5194/gmd-12-1643-2019, 2019.

Thomas, M. A., Wyser, K., Wang, S., Chatziparaschos, M., Georgakaki, P., Costa-Surós, M., Gonçalves Ageitos, M., Kanakidou, M., García-Pando, C. P., Nenes, A., van Noije, T., Le Sager, P., and Devasthale, A.: Recent improvements and maximum covariance analysis of aerosol and cloud properties in the EC-Earth3-AerChem model, Geosci. Model Dev., 17, 6903–6927, https://doi.org/10.5194/gmd-17-6903-2024, 2024.

Tsimpidi, A. P., Karydis, V. A., Pozzer, A., Pandis, S. N., and Lelieveld, J.: ORACLE (v1.0): module to simulate the organic aerosol composition and evolution in the atmosphere, Geosci. Model Dev., 7, 3153–3172, https://doi.org/10.5194/gmd-7-3153-2014, 2014.

van Marle, M. J. E., Kloster, S., Magi, B. I., Marlon, J. R., Daniau, A.-L., Field, R. D., Arneth, A., Forrest, M., Hantson, S., Kehrwald, N. M., Knorr, W., Lasslop, G., Li, F., Mangeon, S., Yue, C., Kaiser, J. W., and van der Werf, G. R.: Historic global biomass burning emissions for CMIP6 (BB4CMIP) based on merging satellite observations with proxies and fire models (1750–2015), Geosci. Model Dev., 10, 3329–3357, https://doi.org/10.5194/gmd-10-3329-2017, 2017.

van Noije, T., Bergman, T., Le Sager, P., O'Donnell, D., Makkonen, R., Gonçalves-Ageitos, M., Döscher, R., Fladrich, U., von Hardenberg, J., Keskinen, J.-P., Korhonen, H., Laakso, A., Myriokefalitakis, S., Ollinaho, P., Pérez García-Pando, C., Reerink, T., Schrödner, R., Wyser, K., and Yang, S.: EC-Earth3-AerChem: a global climate model with interactive aerosols and atmospheric chemistry participating in CMIP6 , Geosci. Model Dev., 14, 5637–5668, https://doi.org/10.5194/gmd-14-5637-2021, 2021.

Vehkamäki, H., Kulmala, M., Napari, I., Lehtinen, K. E. J., Timmreck, C., Noppel, M., and Laaksonen, A.: An improved parameterization for sulfuric acid–water nucleation rates for tropospheric and stratospheric conditions, J. Geophys. Res., 107, 4622, https://doi.org/10.1029/2002JD002184, 2002.

Veres, P. R., Neuman, J. A., Bertram, T. H., Assaf, E., Wolfe, G. M., Williamson, C. J., Weinzierl, B., Tilmes, S., Thompson, C. R., Thames, A. B., Schroder, J. C., Saiz-Lopez, A., Rollins, A. W., Roberts, J. M., Price, D., Peischl, J., Nault, B. A., Møller, K. H., Miller, D. O., Meinardi, S., Li, Q., Lamarque, J.-F., Kupc, A., Kjaergaard, H. G., Kinnison, D., Jimenez, J. L., Jernigan, C. M., Hornbrook, R. S., Hills, A., Dollner, M., Day, D. A., Cuevas, C. A., Campuzano-Jost, P., Burkholder, J., Bui, T. P., Brune, W. H., Brown, S. S., Brock, C. A., Bourgeois, I., Blake, D. R., Apel, E. C., and Ryerson, T. B.: Global airborne sampling reveals a previously unobserved dimethyl sulfide oxidation mechanism in the marine atmosphere, Proc. Natl. Acad. Sci., 117, 4505–4510, https://doi.org/10.1073/pnas.1919344117, 2020.

Vignati, E., Wilson, J., and Stier, P.: M7: An efficient size-resolved aerosol microphysics module for large-scale aerosol transport models, J. Geophys. Res., 109, D22202, https://doi.org/10.1029/2003JD004485, 2004.

Williams, J. E. ., Huijnen, V., Bouarar, I., Meziane, M., Schreurs, T., Pelletier, S., Marécal, V., Josse, B., and Flemming, J.: Regional evaluation of the performance of the global CAMS chemical modeling system over the United States (IFS cycle 47r1), Geosci. Model Dev., 15, 4657–4687, https://doi.org/10.5194/gmd-15-4657-2022, 2022.

Zhang, K., O'Donnell, D., Kazil, J., Stier, P., Kinne, S., Lohmann, U., Ferrachat, S., Croft, B., Quaas, J., Wan, H., Rast, S., and Feichter, J.: The global aerosol-climate model ECHAM-HAM, version 2: sensitivity to improvements in process representations, Atmos. Chem. Phys., 12, 8911–8949, https://doi.org/10.5194/acp-12-8911-2012, 2012.